



Crystal structure and Hirshfeld surface analysis of (*E*)-4-({2,2-dichloro-1-[4-(dimethylamino)phenyl]ethenyl}diazenyl)benzonitrile

Namiq Q. Shikhaliyev,^a Zeliha Atioğlu,^b Mehmet Akkurt,^c Gulnar T. Suleymanova,^a Gulnare V. Babayeva^a and Sixberth Mlowe^{d*}

Received 23 August 2021
Accepted 3 September 2021

Edited by L. Van Meervelt, Katholieke Universiteit Leuven, Belgium

Keywords: crystal structure; C—H...N interactions; C—Cl... π interactions; π – π stacking interactions; Hirshfeld surface analysis.

CCDC reference: 2107472

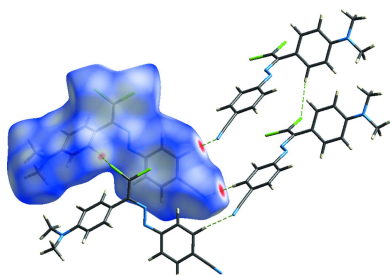
Supporting information: this article has supporting information at journals.iucr.org/e

^aOrganic Chemistry Department, Baku State University, Z. Khalilov str. 23, AZ 1148 Baku, Azerbaijan, ^bDepartment of Aircraft Electrics and Electronics, School of Applied Sciences, Cappadocia University, Mustafapaşa, 50420 Ürgüp, Nevşehir, Turkey, ^cDepartment of Physics, Faculty of Sciences, Erciyes University, 38039 Kayseri, Turkey, and ^dUniversity of Dar es Salaam, Dar es Salaam University College of Education, Department of Chemistry, PO Box 2329, Dar es Salaam, Tanzania. *Correspondence e-mail: sixberth.mlowe@duce.ac.tz

In the title compound, C₁₇H₁₄Cl₂N₄, the dihedral angle between the aromatic rings is 50.09 (9)°. The central –N=N– unit shows an *E* configuration. In the crystal, C—H...N interactions, C—Cl... π and π – π stacking interactions [centroid-to-centroid distance = 3.7719 (14) Å] link the molecules, forming molecular layers approximately parallel to the (002) plane. Additional weak van der Waals interactions between the layers consolidate the three-dimensional packing. Hirshfeld surface analysis indicates that the most important contributions for the crystal packing are from H...H (33.6%), N...H/H...N (17.2%), Cl...H/H...Cl (14.1%) and C...H/H...C (14.1%) contacts.

1. Chemical context

Azo dyes find numerous applications in a diversity of areas, including in molecular recognition, optical data storage, non-linear optics and as molecular switches, antimicrobial agents, colour-changing materials, liquid crystals, dye-sensitized solar cells, mainly because of the ability for *cis*-to-*trans* isomerization and the chromophoric properties of the –N=N– synthon (Maharramov *et al.*, 2018; Viswanathan *et al.*, 2019). Not only isomerization, but azo-hydrazone tautomerism is also an important phenomenon in the coordination chemistry of azo dyes (Mahmoudi *et al.*, 2018*a,b*). Modification of azo dyes with functional groups leads to multifunctional ligands, of which the corresponding metal complexes are effective catalysts in oxidation and in C–C coupling reactions (Ma *et al.*, 2020, 2021; Mahmudov *et al.*, 2013; Mizar *et al.*, 2012). Moreover, the functional properties of azo dyes are dependent on non-covalent bond-donor or -acceptor site(s) attached to the –N=N– synthon (Gurbanov *et al.*, 2020*a,b*; Kopylovich *et al.*, 2011; Mahmudov *et al.*, 2020; Shixaliyev *et al.*, 2014). Thus, we have introduced halogen-bond-donor centres to the –N=N– moiety, leading to a new azo dye, (*E*)-4-({2,2-dichloro-1-[4-(dimethylamino)phenyl]ethenyl}diazenyl)benzonitrile, which provides multiple intermolecular non-covalent interactions.



2. Structural commentary

The aromatic rings C3–C8 and C11–C16 of the title compound (Fig. 1) form a dihedral angle of 50.09 (9)°. In the dimethyl-

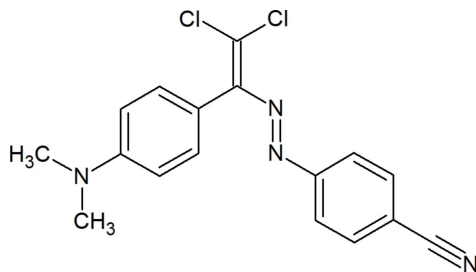


Table 1
Hydrogen-bond geometry (Å, °).

$D-H\cdots A$	$D-H$	$H\cdots A$	$D\cdots A$	$D-H\cdots A$
$C13-H13\cdots N4^i$	0.95	2.48	3.428 (3)	175

Symmetry code: (i) $-x + \frac{5}{2}, y + \frac{1}{2}, -z + \frac{1}{2}$.

amino group, the sum of bond angles about N3 is 357.02° and the nitrogen atom has a flattened trigonal-pyramidal conformation. The atoms of the dimethylamino group and those of its attached benzene ring (C3–C8) are nearly coplanar, with maximum deviations of -0.058 (2), 0.179 (2), and 0.087 (2) Å for N3, C9 and C10, respectively. The title molecule adopts an *E* configuration with respect to the $N1=N2$ bond. The N1/N2/C1–C3/C11/C12 unit is approximately planar with a maximum deviation of 0.102 (2) Å, and makes dihedral angles of 55.44 (9) and 5.36 (9)°, respectively, with the C3–C8 and C11–C16 benzene rings.



3. Supramolecular features and Hirshfeld surface analysis

In the crystal, molecules are linked by $C-H\cdots N$ interactions (Table 1), $C-H\cdots\pi$ [$Cl2\cdots Cg2^{ii} = 3.3910$ (12) Å, $C2\cdots Cg2^{ii} = 3.858$ (2) Å, $C2-Cl2\cdots Cg2^{ii} = 92.07$ (7)°; symmetry code: (ii) $x, 1 + y, z$; where $Cg2$ is the centroid of the C11–C16 benzene ring] and $\pi-\pi$ stacking interactions [$Cg2\cdots Cg1^{iii} = 3.7719$ (14) Å, slippage = 1.741 Å; $Cg1\cdots Cg2^{iv} = 3.7719$ (14) Å, slippage = 1.336 Å; symmetry codes: (iii) $\frac{3}{2} - x, -\frac{1}{2} + y, \frac{1}{2} - z$; (iv) $\frac{3}{2} - x, \frac{1}{2} + y, \frac{1}{2} - z$; where $Cg1$ and $Cg2$ are

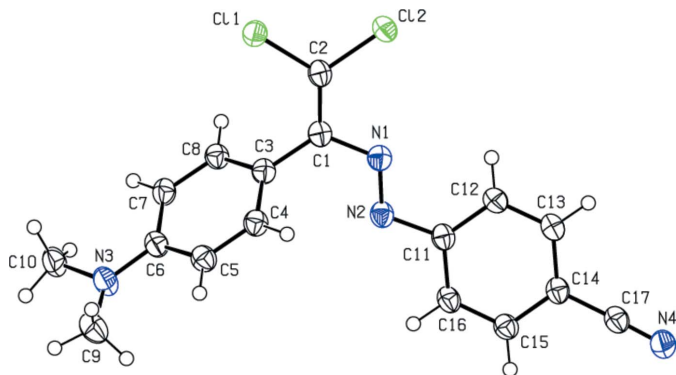


Figure 1
The molecular structure of the title compound, showing the atom labelling and displacement ellipsoids drawn at the 50% probability level.

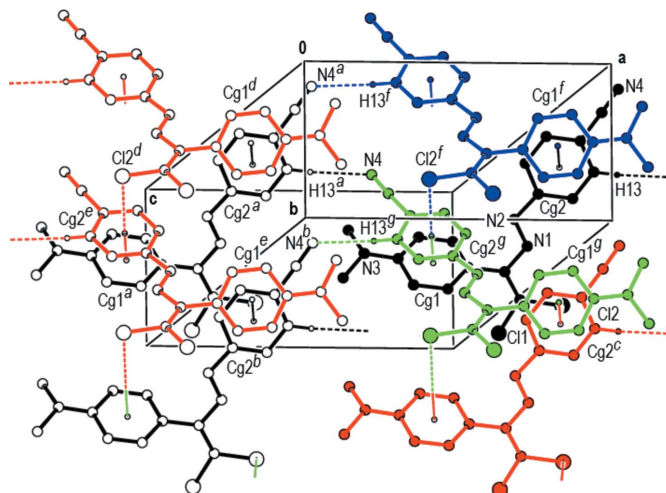


Figure 2
A general view of the $C-H\cdots N$ contacts, $C-Cl\cdots\pi$ interactions and $\pi-\pi$ stacking interactions in the crystal packing of the title compound [symmetry codes: (a) $-1 + x, y, z$; (b) $-1 + x, 1 + y, z$; (c) $x, 1 + y, z$; (d) $\frac{1}{2} - x, -\frac{1}{2} + y, \frac{1}{2} - z$; (e) $\frac{1}{2} - x, \frac{1}{2} + y, \frac{1}{2} - z$; (f) $\frac{3}{2} - x, -\frac{1}{2} + y, \frac{1}{2} - z$; (g) $\frac{3}{2} - x, \frac{1}{2} + y, \frac{1}{2} - z$].

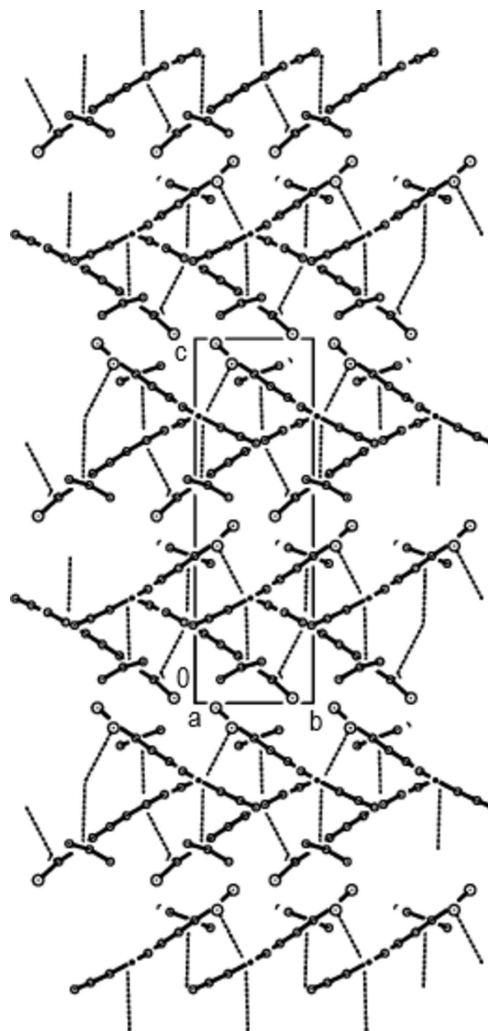


Figure 3
The crystal packing of the title compound, viewed along the a axis, showing the $C-Cl\cdots\pi$ interactions and $\pi-\pi$ stacking interactions as dashed lines.

Table 2
Summary of short interatomic contacts (Å) in the title compound.

Contact	Distance	Symmetry operation
C11...H4	2.86	$x, 1 + y, z$
Cl2...Cl1	3.60	$2 - x, 3 - y, 1 - z$
H9C...C7	2.95	$1 - x, 2 - y, 1 - z$
Cl2...H10B	3.01	$1 + x, y, z$
C2...C2	3.47	$2 - x, 2 - y, 1 - z$
N4...H13	2.48	$-x, -\frac{1}{3} + y, \frac{1}{2} - z$
N4...H7	2.70	$-x, -\frac{2}{3} + y, \frac{1}{2} - z$

centroids of the C3–C8 and C11–C16 benzene rings, respectively], forming molecular layers approximately parallel to the (002) plane with the molecules having a bellows-like shape when viewed along the *a* axis (Figs. 2 and 3). Weak van der Waals interactions between these layers increase the stability of the crystal structure.

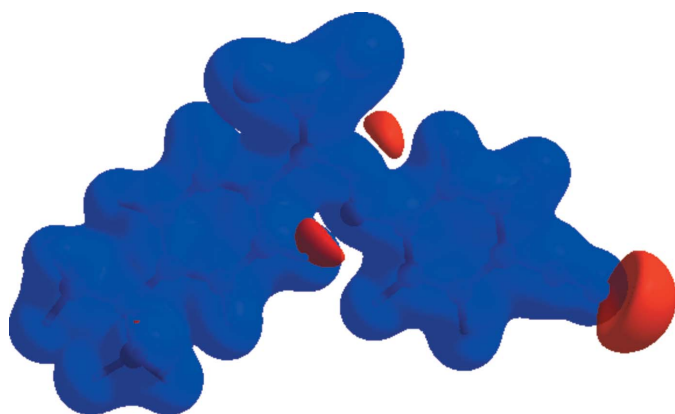


Figure 4
View of the three-dimensional Hirshfeld surface of the title compound plotted over electrostatic potential in the range -0.0500 to 0.0500 a.u. using the STO-3 G basis set at the Hartree–Fock level of theory. Hydrogen-bond donors and acceptors are shown as blue and red regions, respectively, around the atoms, corresponding to positive and negative potentials.

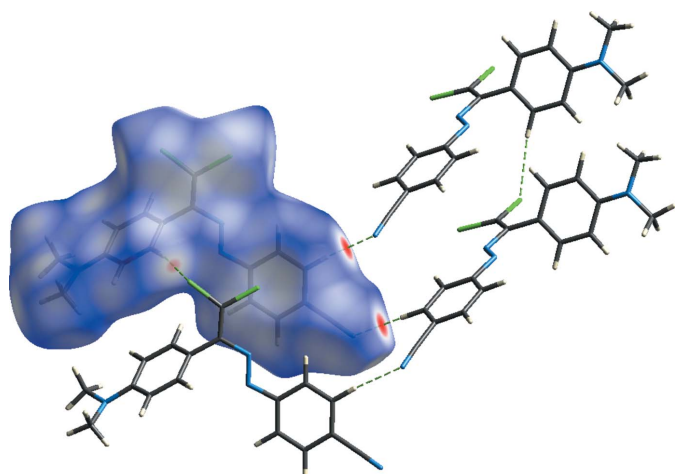
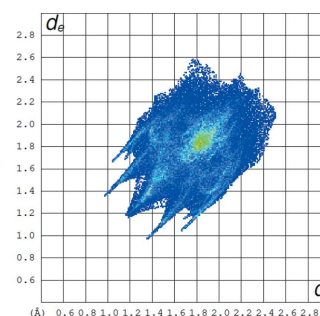
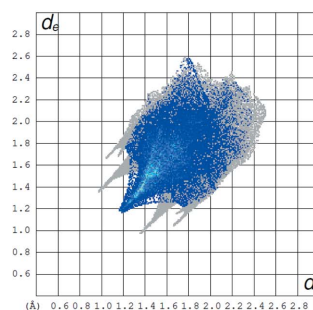


Figure 5
Hirshfeld surface mapped over d_{norm} highlighting the regions of C–H...Cl and C–H...N intermolecular contacts.

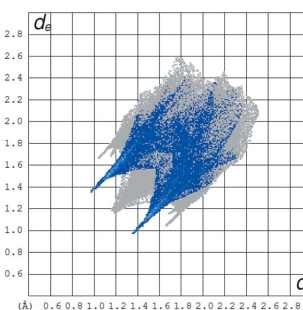
To visualize the intermolecular interactions in the title molecule, *CrystalExplorer17* (Turner *et al.*, 2017) was used to compute Hirshfeld surfaces (McKinnon *et al.*, 2007) and their corresponding two-dimensional fingerprint plots (Spackman & McKinnon, 2002). The Hirshfeld surface mapped over electrostatic potential (Spackman *et al.*, 2008) is shown in Fig. 4. The positive electrostatic potential (blue region) over the surface indicates hydrogen-bond donors, whereas the hydrogen-bond acceptors are represented by a negative electrostatic potential (red region). In the Hirshfeld surface mapped over d_{norm} (Fig. 5), the bright-red spots near atoms H7, H13, N4 and Cl1 indicate the short C–H...N and C–H...Cl contacts (Table 2). Other contacts are equal to or longer than the sum of van der Waals radii. The most important interaction is H...H, contributing 33.6% to the overall crystal packing, which is reflected in Fig. 6*b* as widely scattered



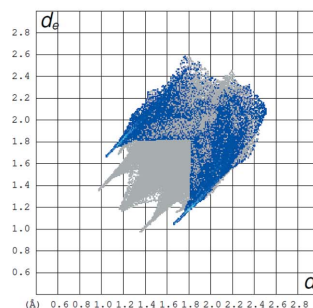
(a) All...All



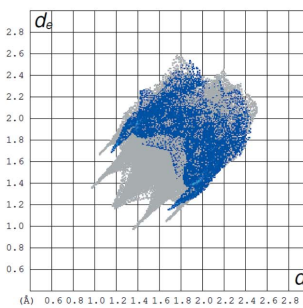
(b) H...H



(c) N...H/H...N



(d) Cl...H/H...Cl



(e) C...H/H...C

Figure 6
(a) The full two-dimensional fingerprint plot for the title compound and those delineated into (b) H...H (33.6%), (c) N...H/H...N (17.2%), (d) Cl...H/H...Cl (14.1%) and (e) C...H/H...C (14.1%) contacts.

Table 3

Percentage contributions of interatomic contacts to the Hirshfeld surface for the title compound.

Contact	Percentage contribution
H...H	33.6
N...H/H...N	17.2
Cl...H/H...Cl	14.1
C...H/H...C	14.1
C...C	6.7
Cl...C/C...Cl	6.3
Cl...Cl	3.5
Cl...N/N...Cl	2.5
N...C/C...N	1.9
N...N	0.1

points of high density due to the large hydrogen content of the molecule, with the tip at $d_e = d_i = 1.15$ Å. The reciprocal N...H/H...N interactions appear as two symmetrical broad wings with $d_e + d_i = 2.3$ Å and contribute 17.2% to the Hirshfeld surface (Fig. 6c). The reciprocal Cl...H/H...Cl interactions (14.1% contribution) are present as two symmetrical broad wings with $d_e + d_i = 2.7$ (Fig. 6d). The pair of characteristic wings in the fingerprint plot delineated into H...C/C...H contacts (Fig. 6e; 14.1% contribution) have the tips at $d_e + d_i = 2.8$ Å. The smaller percentage contributions to the Hirshfeld surface from the various other interatomic contact are comparatively listed in Table 3.

4. Database survey

A search of the Cambridge Structural Database (CSD, Version 5.40, update November 2018; Groom *et al.*, 2016) for structures having an (*E*)-1-(2,2-dichloro-1-phenylethenyl)-2-phenyldiazene unit gave 25 hits. Six compounds closely resemble the title compound, *viz.* 4-{2,2-dichloro-1-[(*E*)-2-(4-methylphenyl)diazene-1-yl]ethenyl}-*N,N*-dimethylaniline [(I); Özkaraça *et al.*, 2020], 4-{2,2-dichloro-1-[(*E*)-(4-fluorophenyl)diazene]ethenyl}-*N,N*-dimethylaniline [(II); Özkaraça *et al.*, 2020], 1-(4-chlorophenyl)-2-[2,2-dichloro-1-(4-fluorophenyl)ethenyl]diazene [(III); Shikhaliyev *et al.*, 2019], 1-(4-bromophenyl)-2-[2,2-dichloro-1-(4-nitrophenyl)ethenyl]diazene [(IV); Akkurt *et al.*, 2019], 1-(4-chlorophenyl)-2-[2,2-dichloro-1-(4-nitrophenyl)ethenyl]diazene [(V); Akkurt *et al.*, 2019] and 1-[2,2-dichloro-1-(4-nitrophenyl)ethenyl]-2-(4-fluorophenyl)diazene [(VI); Atioğlu *et al.*, 2019].

In the crystal of (I), molecules are linked by pairs of C—Cl... π interactions, forming inversion dimers. A short intermolecular Cl...Cl contact [3.2555 (9) Å] links the dimers, forming a ribbon along the *c*-axis direction. The crystal structure of (II) is stabilized by C—Cl... π and van der Waals interactions. In (III), molecules are stacked in columns along the *a* axis *via* weak C—H...Cl hydrogen bonds and face-to-face π — π stacking interactions. The crystal packing is further stabilized by short Cl...Cl contacts. In the crystals of (IV) and (V), molecules are linked through weak X...Cl contacts [*X* = Br for (IV) and Cl for (V)] and C—H...Cl and C—Cl... π interactions into sheets parallel to the *ab* plane. In (VI), molecules are linked by C—H...O hydrogen bonds into

Table 4

Experimental details.

Crystal data	
Chemical formula	C ₁₇ H ₁₄ Cl ₂ N ₄
<i>M_r</i>	345.22
Crystal system, space group	Monoclinic, <i>P</i> 2 ₁ / <i>n</i>
Temperature (K)	100
<i>a</i> , <i>b</i> , <i>c</i> (Å)	12.396 (3), 6.5280 (7), 20.758 (3)
β (°)	104.39 (2)
<i>V</i> (Å ³)	1627.1 (5)
<i>Z</i>	4
Radiation type	Synchrotron, $\lambda = 0.79475$ Å
μ (mm ⁻¹)	0.54
Crystal size (mm)	0.10 × 0.08 × 0.05
Data collection	
Diffractometer	Rayonix SX165 CCD
Absorption correction	Multi-scan (SCALA; Evans, 2006)
<i>T_{min}</i> , <i>T_{max}</i>	0.939, 0.966
No. of measured, independent and observed [<i>I</i> > 2 σ (<i>I</i>)] reflections	21540, 3712, 2913
<i>R_{int}</i>	0.066
(<i>sin</i> θ / λ) _{max} (Å ⁻¹)	0.648
Refinement	
<i>R</i> [<i>F</i> ² > 2 σ (<i>F</i> ²)], <i>wR</i> (<i>F</i> ²), <i>S</i>	0.040, 0.110, 1.06
No. of reflections	3712
No. of parameters	211
H-atom treatment	H-atom parameters constrained
$\Delta\rho_{max}$, $\Delta\rho_{min}$ (e Å ⁻³)	0.34, -0.36

Computer programs: *Marccd* (Doyle, 2011), *iMosflm* (Battye *et al.*, 2011), *SHELXT* (Sheldrick, 2015a), *SHELXL* (Sheldrick, 2015b), *ORTEP-3 for Windows* (Farrugia, 2012) and *PLATON* (Spek, 2020).

zigzag chains running along the *c*-axis direction. The crystal packing is further stabilized by C—Cl... π , C—F... π and N—O... π interactions.

5. Synthesis and crystallization

The title compound was synthesized according to a reported method (Shikhaliyev *et al.*, 2018, 2019). A 20 mL screw-neck vial was charged with DMSO (10 mL), (*Z*)-4-{2-[4-(dimethylamino)benzylidene]hydrazinyl}benzotrile (264 mg, 1 mmol), tetramethylethylenediamine (TMEDA) (295 mg, 2.5 mmol), CuCl (2 mg, 0.02 mmol) and CCl₄ (20 mmol, 10 equiv). After 1–3 h (until TLC analysis showed complete consumption of the corresponding Schiff base), the reaction mixture was poured into ~0.01 *M* solution of HCl (100 mL, pH = 2–3), and extracted with dichloromethane (3 × 20 mL). The combined organic phase was washed with water (3 × 50 mL) and brine (30 mL), dried over anhydrous Na₂SO₄ and concentrated using a vacuum rotary evaporator. The residue was purified by column chromatography on silica gel using appropriate mixtures of hexane and dichloromethane (3/1–1/1). Crystals suitable for X-ray analysis were obtained by slow evaporation of an ethanol solution. Colourless solid (69%); m.p. 395 K. Analysis calculated for C₁₇H₁₄Cl₂N₄: C 59.15, H 4.09, N 16.23%; found: C 59.05, H 4.02, N 16.19%. ¹H NMR (300 MHz, CDCl₃) δ 3.04 (6H, NMe₂), 6.75–7.89 (8H, Ar). ¹³C NMR (75 MHz, CDCl₃) δ 162.08, 154.31, 152.59, 146.76, 135.98, 132.50, 131.25, 128.75, 120.90, 117.76, 115.52 and 38.42. ESI-MS: *m/z*: 346.18 [*M* + H]⁺.

6. Refinement

Crystal data, data collection and structure refinement details are summarized in Table 4. The C-bound H atoms were positioned geometrically and treated as riding atoms, C–H = 0.95 Å with $U_{\text{iso}}(\text{H}) = 1.2U_{\text{eq}}(\text{C})$ for aromatic H atoms and C–H = 0.98 Å with $U_{\text{iso}}(\text{H}) = 1.5U_{\text{eq}}(\text{C})$ for methyl H atoms.

Acknowledgements

The authors' contributions are as follows. Conceptualization, NQS, MA and SM; synthesis, GTS and GVB; X-ray analysis, ZA and MA; writing (review and editing of the manuscript), funding acquisition, NQS, GTS and GVB; supervision, NQS, MA and SM.

Funding information

This work was performed under the support of the Science Development Foundation under the President of the Republic of Azerbaijan (grant No. EIF-BGM-4- RFTF-1/2017–21/13/4).

References

Akkurt, M., Shikhaliyev, N. Q., Suleymanova, G. T., Babayeva, G. V., Mammadova, G. Z., Niyazova, A. A., Shikhaliyeva, I. M. & Toze, F. A. A. (2019). *Acta Cryst.* **E75**, 1199–1204.

Atioğlu, Z., Akkurt, M., Shikhaliyev, N. Q., Suleymanova, G. T., Bagirova, K. N. & Toze, F. A. A. (2019). *Acta Cryst.* **E75**, 237–241.

Battye, T. G. G., Kontogiannis, L., Johnson, O., Powell, H. R. & Leslie, A. G. W. (2011). *Acta Cryst.* **D67**, 271–281.

Doyle, R. A. (2011). *Merccid software manual*. Rayonix LLC, Evanston, IL 60201, USA.

Evans, P. (2006). *Acta Cryst.* **D62**, 72–82.

Farrugia, L. J. (2012). *J. Appl. Cryst.* **45**, 849–854.

Groom, C. R., Bruno, I. J., Lightfoot, M. P. & Ward, S. C. (2016). *Acta Cryst.* **B72**, 171–179.

Gurbanov, A. V., Kuznetsov, M. L., Demukhamedova, S. D., Alieva, I. N., Godjaev, N. M., Zubkov, F. I., Mahmudov, K. T. & Pombeiro, A. J. L. (2020a). *CrystEngComm*, **22**, 628–633.

Gurbanov, A. V., Kuznetsov, M. L., Mahmudov, K. T., Pombeiro, A. J. L. & Resnati, G. (2020b). *Chem. Eur. J.* **26**, 14833–14837.

Kopylovich, M. N., Mahmudov, K. T., Mizar, A. & Pombeiro, A. J. L. (2011). *Chem. Commun.* **47**, 7248–7250.

Ma, Z., Mahmudov, K. T., Aliyeva, V. A., Gurbanov, A. V., Guedes da Silva, M. F. C. & Pombeiro, A. J. L. (2021). *Coord. Chem. Rev.* **437**, 213859.

Ma, Z., Mahmudov, K. T., Aliyeva, V. A., Gurbanov, A. V. & Pombeiro, A. J. L. (2020). *Coord. Chem. Rev.* **423**, 213482.

Maharramov, A. M., Shikhaliyev, N. Q., Suleymanova, G. T., Gurbanov, A. V., Babayeva, G. V., Mammadova, G. Z., Zubkov, F. I., Nenajdenko, V. G., Mahmudov, K. T. & Pombeiro, A. J. L. (2018). *Dyes Pigments*, **159**, 135–141.

Mahmoudi, G., Afkhami, F. A., Castiñeiras, A., García-Santos, I., Gurbanov, A., Zubkov, F. I., Mitoraj, M. P., Kukułka, M., Sagan, F., Szczepanik, D. W., Konyaeva, I. A. & Safin, D. A. (2018a). *Inorg. Chem.* **57**, 4395–4408.

Mahmoudi, G., Zangrando, E., Mitoraj, M. P., Gurbanov, A. V., Zubkov, F. I., Moosavifar, M., Konyaeva, I. A., Kirillov, A. M. & Safin, D. A. (2018b). *New J. Chem.* **42**, 4959–4971.

Mahmudov, K. T., Gurbanov, A. V., Aliyeva, V. A., Resnati, G. & Pombeiro, A. J. L. (2020). *Coord. Chem. Rev.* **418**, 213381.

Mahmudov, K. T., Kopylovich, M. N., Haukka, M., Mahmudova, G. S., Esmaeila, E. F., Chyragov, F. M. & Pombeiro, A. J. L. (2013). *J. Mol. Struct.* **1048**, 108–112.

McKinnon, J. J., Jayatilaka, D. & Spackman, M. A. (2007). *Chem. Commun.* pp. 3814–3816.

Mizar, A., Guedes da Silva, M. F. C., Kopylovich, M. N., Mukherjee, S., Mahmudov, K. T. & Pombeiro, A. J. L. (2012). *Eur. J. Inorg. Chem.* pp. 2305–2313.

Özkaraca, K., Akkurt, M., Shikhaliyev, N. Q., Askerova, U. F., Suleymanova, G. T., Shikhaliyeva, I. M. & Bhattarai, A. (2020). *Acta Cryst.* **E76**, 811–815.

Sheldrick, G. M. (2015a). *Acta Cryst.* **A71**, 3–8.

Sheldrick, G. M. (2015b). *Acta Cryst.* **C71**, 3–8.

Shikhaliyev, N. Q., Ahmadova, N. E., Gurbanov, A. V., Maharramov, A. M., Mammadova, G. Z., Nenajdenko, V. G., Zubkov, F. I., Mahmudov, K. T. & Pombeiro, A. J. L. (2018). *Dyes Pigments*, **150**, 377–381.

Shikhaliyev, N. Q., Çelikesir, S. T., Akkurt, M., Bagirova, K. N., Suleymanova, G. T. & Toze, F. A. A. (2019). *Acta Cryst.* **E75**, 465–469.

Shikhaliyev, N. Q., Kuznetsov, M. L., Maharramov, A. M., Gurbanov, A. V., Ahmadova, N. E., Nenajdenko, V. G., Mahmudov, K. T. & Pombeiro, A. J. L. (2019). *CrystEngComm*, **21**, 5032–5038.

Shixaliyev, N. Q., Gurbanov, A. V., Maharramov, A. M., Mahmudov, K. T., Kopylovich, M. N., Martins, L. M. D. R. S., Muzalevskiy, V. M., Nenajdenko, V. G. & Pombeiro, A. J. L. (2014). *New J. Chem.* **38**, 4807–4815.

Spackman, M. A. & McKinnon, J. J. (2002). *CrystEngComm*, **4**, 378–392.

Spackman, M. A., McKinnon, J. J. & Jayatilaka, D. (2008). *CrystEngComm*, **10**, 377–388.

Spek, A. L. (2020). *Acta Cryst.* **E76**, 1–11.

Turner, M. J., McKinnon, J. J., Wolff, S. K., Grimwood, D. J., Spackman, P. R., Jayatilaka, D. & Spackman, M. A. (2017). *CrystalExplorer17*. The University of Western Australia.

Viswanathan, A., Kute, D., Musa, A., Mani, S. K., Sipilä, V., Emmert-Streib, F., Zubkov, F. I., Gurbanov, A. V., Yli-Harja, O. & Kandhavelu, M. (2019). *Eur. J. Med. Chem.* **166**, 291–303.

supporting information

Acta Cryst. (2021). E77, 994-998 [https://doi.org/10.1107/S2056989021009154]

Crystal structure and Hirshfeld surface analysis of (*E*)-4-({2,2-dichloro-1-[4-(dimethylamino)phenyl]ethenyl}diazenyl)benzotrile

Namiq Q. Shikhaliyev, Zeliha Atioğlu, Mehmet Akkurt, Gulnar T. Suleymanova, Gulnare V. Babayeva and Sixberth Mlowe

Computing details

Data collection: *Marccd* (Doyle, 2011); cell refinement: *iMosflm* (Battye *et al.*, 2011); data reduction: *iMosflm* (Battye *et al.*, 2011); program(s) used to solve structure: SHELXT (Sheldrick, 2015a); program(s) used to refine structure: *SHELXL* (Sheldrick, 2015b); molecular graphics: *ORTEP-3 for Windows* (Farrugia, 2012); software used to prepare material for publication: *PLATON* (Spek, 2020).

(*E*)-4-({2,2-Dichloro-1-[4-(dimethylamino)phenyl]ethenyl}diazenyl)benzotrile

Crystal data

$C_{17}H_{14}Cl_2N_4$

$M_r = 345.22$

Monoclinic, $P2_1/n$

$a = 12.396$ (3) Å

$b = 6.5280$ (7) Å

$c = 20.758$ (3) Å

$\beta = 104.39$ (2)°

$V = 1627.1$ (5) Å³

$Z = 4$

$F(000) = 712$

$D_x = 1.409$ Mg m⁻³

Synchrotron radiation, $\lambda = 0.79475$ Å

Cell parameters from 600 reflections

$\theta = 2.0$ – 28.0 °

$\mu = 0.54$ mm⁻¹

$T = 100$ K

Prism, colourless

$0.10 \times 0.08 \times 0.05$ mm

Data collection

Rayonix SX165 CCD
diffractometer

/f scan

Absorption correction: multi-scan
(*SCALA*; Evans, 2006)

$T_{\min} = 0.939$, $T_{\max} = 0.966$

21540 measured reflections

3712 independent reflections

2913 reflections with $I > 2\sigma(I)$

$R_{\text{int}} = 0.066$

$\theta_{\max} = 31.0$ °, $\theta_{\min} = 2.0$ °

$h = -16 \rightarrow 16$

$k = -8 \rightarrow 8$

$l = -25 \rightarrow 26$

Refinement

Refinement on F^2

Least-squares matrix: full

$R[F^2 > 2\sigma(F^2)] = 0.040$

$wR(F^2) = 0.110$

$S = 1.06$

3712 reflections

211 parameters

0 restraints

Primary atom site location: difference Fourier
map

Secondary atom site location: difference Fourier
map

Hydrogen site location: inferred from
neighbouring sites

H-atom parameters constrained

$w = 1/[\sigma^2(F_o^2) + (0.0535P)^2 + 0.5596P]$

where $P = (F_o^2 + 2F_c^2)/3$

$$(\Delta/\sigma)_{\max} < 0.001$$

$$\Delta\rho_{\max} = 0.34 \text{ e } \text{\AA}^{-3}$$

$$\Delta\rho_{\min} = -0.36 \text{ e } \text{\AA}^{-3}$$

Extinction correction: SHELXL,
 $\text{Fc}^* = k\text{Fc}[1 + 0.001x\text{Fc}^2\lambda^3/\sin(2\theta)]^{-1/4}$
 Extinction coefficient: 0.0082 (8)

Special details

Geometry. All esds (except the esd in the dihedral angle between two l.s. planes) are estimated using the full covariance matrix. The cell esds are taken into account individually in the estimation of esds in distances, angles and torsion angles; correlations between esds in cell parameters are only used when they are defined by crystal symmetry. An approximate (isotropic) treatment of cell esds is used for estimating esds involving l.s. planes.

Fractional atomic coordinates and isotropic or equivalent isotropic displacement parameters (\AA^2)

	x	y	z	$U_{\text{iso}}^*/U_{\text{eq}}$
Cl1	0.88106 (4)	1.32286 (7)	0.48668 (2)	0.03392 (14)
Cl2	1.05932 (4)	1.18867 (7)	0.43125 (2)	0.03201 (14)
N1	0.91524 (13)	0.8624 (3)	0.37007 (8)	0.0292 (3)
N2	0.85729 (13)	0.7167 (3)	0.33932 (8)	0.0300 (3)
N3	0.40040 (13)	0.8913 (3)	0.40216 (9)	0.0380 (4)
N4	1.13398 (14)	-0.0162 (3)	0.21331 (9)	0.0398 (4)
C1	0.85825 (15)	0.9987 (3)	0.40327 (9)	0.0284 (4)
C2	0.92392 (15)	1.1508 (3)	0.43572 (9)	0.0295 (4)
C3	0.73981 (15)	0.9728 (3)	0.40425 (9)	0.0291 (4)
C4	0.70143 (15)	0.7904 (3)	0.42580 (9)	0.0310 (4)
H4	0.7525	0.6816	0.4404	0.037*
C5	0.59082 (16)	0.7638 (3)	0.42649 (10)	0.0330 (4)
H5	0.5678	0.6384	0.4421	0.040*
C6	0.51174 (15)	0.9206 (3)	0.40439 (9)	0.0310 (4)
C7	0.55024 (15)	1.1054 (3)	0.38262 (9)	0.0312 (4)
H7	0.4994	1.2145	0.3678	0.037*
C8	0.66197 (15)	1.1295 (3)	0.38267 (9)	0.0294 (4)
H8	0.6859	1.2551	0.3677	0.035*
C9	0.36642 (18)	0.7158 (4)	0.43561 (12)	0.0434 (5)
H9A	0.3835	0.5892	0.4148	0.065*
H9B	0.2862	0.7231	0.4319	0.065*
H9C	0.4067	0.7169	0.4826	0.065*
C10	0.32281 (16)	1.0620 (4)	0.38642 (11)	0.0410 (5)
H10A	0.3390	1.1609	0.4231	0.061*
H10B	0.2465	1.0113	0.3800	0.061*
H10C	0.3307	1.1290	0.3456	0.061*
C11	0.92081 (15)	0.5780 (3)	0.30993 (9)	0.0291 (4)
C12	1.03445 (15)	0.6030 (3)	0.31285 (9)	0.0315 (4)
H12	1.0731	0.7214	0.3330	0.038*
C13	1.08971 (15)	0.4540 (3)	0.28610 (9)	0.0318 (4)
H13	1.1666	0.4692	0.2878	0.038*
C14	1.03148 (15)	0.2803 (3)	0.25645 (9)	0.0297 (4)
C15	0.91773 (15)	0.2583 (3)	0.25146 (9)	0.0308 (4)
H15	0.8784	0.1423	0.2299	0.037*
C16	0.86290 (15)	0.4084 (3)	0.27846 (9)	0.0308 (4)
H16	0.7855	0.3952	0.2754	0.037*

C17	1.08914 (15)	0.1179 (3)	0.23155 (10)	0.0329 (4)
-----	--------------	------------	--------------	------------

Atomic displacement parameters (Å²)

	U^{11}	U^{22}	U^{33}	U^{12}	U^{13}	U^{23}
C11	0.0306 (2)	0.0350 (3)	0.0359 (3)	0.00155 (18)	0.00763 (19)	-0.00490 (19)
C12	0.0255 (2)	0.0375 (3)	0.0326 (2)	-0.00150 (18)	0.00657 (17)	0.00029 (19)
N1	0.0276 (7)	0.0326 (9)	0.0261 (8)	0.0018 (6)	0.0045 (6)	0.0004 (6)
N2	0.0254 (7)	0.0358 (9)	0.0275 (8)	0.0029 (6)	0.0043 (6)	-0.0011 (7)
N3	0.0275 (8)	0.0428 (10)	0.0457 (10)	0.0004 (7)	0.0126 (7)	0.0039 (8)
N4	0.0316 (8)	0.0444 (11)	0.0441 (10)	0.0004 (8)	0.0109 (7)	-0.0063 (8)
C1	0.0270 (9)	0.0323 (10)	0.0254 (9)	0.0026 (7)	0.0055 (7)	0.0026 (7)
C2	0.0257 (9)	0.0348 (10)	0.0272 (9)	0.0036 (7)	0.0052 (7)	0.0033 (7)
C3	0.0271 (9)	0.0333 (10)	0.0261 (9)	0.0017 (7)	0.0051 (7)	-0.0007 (7)
C4	0.0284 (9)	0.0334 (11)	0.0300 (9)	0.0034 (7)	0.0049 (7)	0.0010 (8)
C5	0.0313 (9)	0.0375 (11)	0.0304 (10)	-0.0013 (8)	0.0081 (8)	0.0007 (8)
C6	0.0258 (9)	0.0384 (11)	0.0289 (9)	-0.0008 (8)	0.0071 (7)	-0.0017 (8)
C7	0.0276 (9)	0.0352 (10)	0.0301 (9)	0.0048 (8)	0.0062 (7)	-0.0010 (8)
C8	0.0269 (9)	0.0326 (10)	0.0277 (9)	0.0013 (7)	0.0053 (7)	0.0000 (8)
C9	0.0360 (11)	0.0539 (14)	0.0430 (12)	-0.0065 (10)	0.0153 (9)	0.0035 (10)
C10	0.0251 (9)	0.0503 (13)	0.0475 (12)	0.0022 (9)	0.0089 (8)	-0.0047 (10)
C11	0.0258 (9)	0.0345 (11)	0.0264 (9)	0.0030 (7)	0.0052 (7)	0.0024 (8)
C12	0.0266 (9)	0.0347 (10)	0.0326 (10)	-0.0018 (8)	0.0064 (7)	0.0001 (8)
C13	0.0255 (9)	0.0388 (11)	0.0317 (10)	-0.0001 (8)	0.0085 (7)	0.0016 (8)
C14	0.0271 (9)	0.0364 (11)	0.0258 (9)	0.0020 (7)	0.0069 (7)	0.0010 (8)
C15	0.0274 (9)	0.0355 (10)	0.0287 (9)	-0.0008 (8)	0.0057 (7)	0.0000 (8)
C16	0.0231 (8)	0.0403 (11)	0.0283 (9)	-0.0002 (8)	0.0052 (7)	-0.0014 (8)
C17	0.0267 (9)	0.0405 (11)	0.0311 (9)	-0.0009 (8)	0.0064 (7)	-0.0002 (9)

Geometric parameters (Å, °)

C11—C2	1.715 (2)	C7—H7	0.9500
C12—C2	1.7217 (19)	C8—H8	0.9500
N1—N2	1.265 (2)	C9—H9A	0.9800
N1—C1	1.417 (2)	C9—H9B	0.9800
N2—C11	1.432 (2)	C9—H9C	0.9800
N3—C6	1.383 (2)	C10—H10A	0.9800
N3—C10	1.456 (3)	C10—H10B	0.9800
N3—C9	1.455 (3)	C10—H10C	0.9800
N4—C17	1.150 (3)	C11—C16	1.391 (3)
C1—C2	1.353 (3)	C11—C12	1.404 (2)
C1—C3	1.483 (2)	C12—C13	1.383 (3)
C3—C4	1.396 (3)	C12—H12	0.9500
C3—C8	1.401 (3)	C13—C14	1.402 (3)
C4—C5	1.386 (3)	C13—H13	0.9500
C4—H4	0.9500	C14—C15	1.395 (3)
C5—C6	1.412 (3)	C14—C17	1.444 (3)
C5—H5	0.9500	C15—C16	1.388 (3)

C6—C7	1.412 (3)	C15—H15	0.9500
C7—C8	1.394 (3)	C16—H16	0.9500
N2—N1—C1	115.36 (15)	N3—C9—H9B	109.5
N1—N2—C11	112.77 (15)	H9A—C9—H9B	109.5
C6—N3—C10	120.00 (18)	N3—C9—H9C	109.5
C6—N3—C9	119.85 (18)	H9A—C9—H9C	109.5
C10—N3—C9	117.17 (17)	H9B—C9—H9C	109.5
C2—C1—N1	113.08 (16)	N3—C10—H10A	109.5
C2—C1—C3	123.52 (17)	N3—C10—H10B	109.5
N1—C1—C3	123.36 (17)	H10A—C10—H10B	109.5
C1—C2—C11	123.19 (15)	N3—C10—H10C	109.5
C1—C2—C12	123.55 (15)	H10A—C10—H10C	109.5
C11—C2—C12	113.26 (11)	H10B—C10—H10C	109.5
C4—C3—C8	117.53 (17)	C16—C11—C12	120.54 (17)
C4—C3—C1	121.25 (17)	C16—C11—N2	115.41 (16)
C8—C3—C1	121.21 (18)	C12—C11—N2	124.03 (17)
C5—C4—C3	121.80 (18)	C13—C12—C11	119.48 (18)
C5—C4—H4	119.1	C13—C12—H12	120.3
C3—C4—H4	119.1	C11—C12—H12	120.3
C4—C5—C6	120.97 (19)	C12—C13—C14	119.54 (17)
C4—C5—H5	119.5	C12—C13—H13	120.2
C6—C5—H5	119.5	C14—C13—H13	120.2
N3—C6—C5	121.14 (18)	C15—C14—C13	121.10 (18)
N3—C6—C7	121.41 (18)	C15—C14—C17	118.60 (18)
C5—C6—C7	117.41 (17)	C13—C14—C17	120.29 (17)
C8—C7—C6	120.71 (18)	C16—C15—C14	118.99 (18)
C8—C7—H7	119.6	C16—C15—H15	120.5
C6—C7—H7	119.6	C14—C15—H15	120.5
C7—C8—C3	121.57 (19)	C15—C16—C11	120.29 (17)
C7—C8—H8	119.2	C15—C16—H16	119.9
C3—C8—H8	119.2	C11—C16—H16	119.9
N3—C9—H9A	109.5	N4—C17—C14	177.5 (2)
C1—N1—N2—C11	-176.74 (15)	C4—C5—C6—C7	-0.9 (3)
N2—N1—C1—C2	179.58 (16)	N3—C6—C7—C8	-177.38 (18)
N2—N1—C1—C3	1.6 (3)	C5—C6—C7—C8	0.5 (3)
N1—C1—C2—C11	-173.44 (13)	C6—C7—C8—C3	-0.1 (3)
C3—C1—C2—C11	4.5 (3)	C4—C3—C8—C7	0.1 (3)
N1—C1—C2—C12	5.4 (2)	C1—C3—C8—C7	179.17 (17)
C3—C1—C2—C12	-176.62 (14)	N1—N2—C11—C16	176.66 (16)
C2—C1—C3—C4	-123.2 (2)	N1—N2—C11—C12	-1.9 (3)
N1—C1—C3—C4	54.5 (3)	C16—C11—C12—C13	-2.2 (3)
C2—C1—C3—C8	57.7 (3)	N2—C11—C12—C13	176.31 (17)
N1—C1—C3—C8	-124.5 (2)	C11—C12—C13—C14	0.0 (3)
C8—C3—C4—C5	-0.4 (3)	C12—C13—C14—C15	2.2 (3)
C1—C3—C4—C5	-179.54 (18)	C12—C13—C14—C17	-176.58 (18)
C3—C4—C5—C6	0.9 (3)	C13—C14—C15—C16	-2.2 (3)

C10—N3—C6—C5	173.06 (19)	C17—C14—C15—C16	176.56 (18)
C9—N3—C6—C5	13.1 (3)	C14—C15—C16—C11	0.0 (3)
C10—N3—C6—C7	-9.1 (3)	C12—C11—C16—C15	2.1 (3)
C9—N3—C6—C7	-169.03 (19)	N2—C11—C16—C15	-176.47 (17)
C4—C5—C6—N3	177.02 (18)		

Hydrogen-bond geometry (Å, °)

<i>D</i> —H \cdots <i>A</i>	<i>D</i> —H	H \cdots <i>A</i>	<i>D</i> \cdots <i>A</i>	<i>D</i> —H \cdots <i>A</i>
C13—H13 \cdots N4 ⁱ	0.95	2.48	3.428 (3)	175

Symmetry code: (i) $-x+5/2, y+1/2, -z+1/2$.